

Density anomaly in a competing interactions lattice gas model

Alan B. de Oliveira

Instituto de Física, Universidade Federal do Rio Grande do Sul, Caixa Postal 15051,
91501-970, Porto Alegre, RS, Brazil

Marcia C. Barbosa[§]

Instituto de Física, Universidade Federal do Rio Grande do Sul, Caixa Postal 15051,
91501-970, Porto Alegre, RS, Brazil

Abstract. We study a very simple model of a short-range attraction and an outer shell repulsion as a test system for demixing phase transition and density anomaly. The phase-diagram is obtained by applying mean field analysis and Monte Carlo simulations to a two dimensional lattice gas with nearest-neighbors attraction and next-nearest-neighbors repulsion (the outer shell). Two liquid phases and density anomaly are found. The coexistence line between these two liquid phases meets a critical line between the fluid and the low density liquid at a tricritical point. The line of maximum density emerges in the vicinity of the tricritical point, close to the demixing transition.

[§] To whom correspondence should be addressed (barbosa@if.ufrgs.br)

1. Introduction

Water is anomalous substance in many respects.

Most liquids contract upon cooling. This is not the case of water, a liquid where the specific volume at ambient pressure starts to increase when cooled below $T = 4^{\circ}\text{C}$ [1]. Besides, in a certain range of pressures, also exhibits an anomalous increase of compressibility and specific heat upon cooling [2]-[4]. It is less well known that water diffuses faster under pressure at very high densities and at very low temperatures [5]. Besides, the viscosity of water decreases upon increasing pressure [6]-[8].

It was proposed a few years ago that these anomalies are related to a second critical point between two liquid phases, a low density liquid (LDL) and a high density liquid (HDL) [9]. This critical point was discovered by computer simulations. This work suggests that this critical point is located at the supercooled region beyond the line of homogeneous nucleation and thus cannot be experimentally measured. Even if this limitation, this hypothesis has been supported by indirect experimental results [7][10].

In spite of the limit of 235K below which water cannot be found in the liquid phase without crystallization, two amorphous phases were observed at much lower temperatures [11]. There is evidence, although yet under test, that these two amorphous phases are related to two liquid phases in fluid water [12][13].

Water is not an isolated case. There are also other examples of tetrahedrally bonded molecular liquids such as phosphorus [14][15] and amorphous silica [16] that also are good candidates for having two liquid phases. Moreover, other materials such as liquid metals [17] and graphite [18] also exhibit thermodynamic anomalies. Unfortunately a coherent and general interpretation of the low density liquid and high density liquid phases is still missing.

What type of potential would be appropriated for describing the tetrahedrally bonded molecular liquids? Directional interactions are certainly an important ingredient in obtaining a quantitative predictions for network-forming liquids like water. However, the models that are obtained from that approach are too complicated, being impossible to go beyond mean field analysis. Isotropic models became the simplest framework to understand the physics of the liquid-liquid phase transition and liquid state anomalies.

Recently it has been shown that the presence of two liquid phases can be associated with a potential with an attractive part and two characteristic short-range repulsive distances. The smallest of these two distances is associated with the hard core of the molecule, while the largest one with the soft core [19]. Acknowledging that core softened (CS) potentials may engender a demixing transition between two liquids of different densities, a number of CS potentials were proposed to model the anisotropic systems described above. The first suggestion was made many years ago by Stell and coworkers in order to explain the isostructural solid-solid transition ending in a critical point [20]-[21]. Debenedetti et al. using general thermodynamic arguments, confirmed that a CS can lead to a coefficient of thermal expansion negative and consequently to density anomaly [22]. This together with the increase of the thermal compressibility has been used as

indications of the presence of two liquid phases [23][24] which may be hidden beyond the homogeneous nucleation. The difficulty with these approaches is that continuous potentials usually lead to crystallization at the region where the critical point would be expected. The analysis of the presence of both the two liquid phases and the critical point becomes indirect.

Nevertheless the apparent success of the CS potentials, it is not clear that the presence of two liquid phases and anomalies are associated only with them [22] or if they result from the presence of two competing scales like the ones present in the CS potentials. In this work we analyze another type of model system where two competing scales are also present. We study a potential with a hard core, a short-range attractive part and a repulsive shell. While the attraction accounts both for the van der Waals and hydrogen bonding interactions, the outer shell repulsion is related to the interstitial molecule that break the tetrahedral structure like the interstitial oxygens in water. In order to circumvent crystallization, our model system is a two dimensional lattice gas with first-neighbors attraction and second neighbors repulsion. The system is in contact with a reservoir of particles.

We show that this very simple system exhibits both density anomaly and two liquid phases. However, instead of having a critical point ending the coexistence line between the two liquid phases as one usually would expect, it has a tricritical point. The connection between the presence of criticality and the density anomaly shown.

The reminder of the paper goes as follows. In sec.(2) the model is presented, the mean field analysis is shown on sec.(3), results from simulations are discussed in sec.(4) and our findings are summarized in sec.(5).

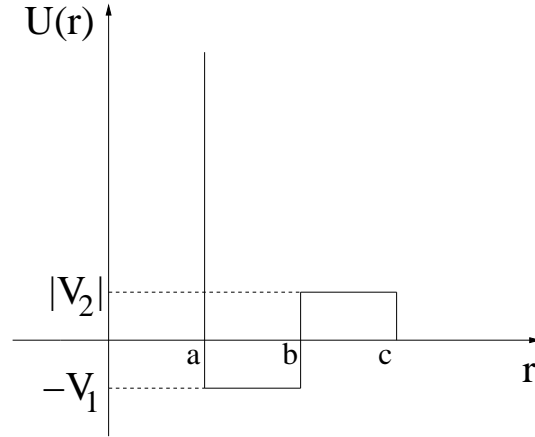
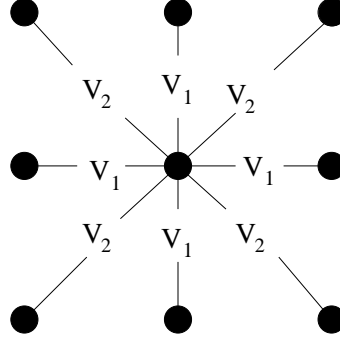
2. The model

Our system is represented by a square lattice with N sites. Associated to each site there is an occupational variable, σ_i . If the site is occupied by molecule, $\sigma_i = 1$, otherwise $\sigma_i = 0$. Each site interacts with its nearest neighbors with attractive interactions and with its next-nearest neighbors with repulsive interactions (see Fig.1). Therefore the Hamiltonian of this system is given by

$$\mathcal{H} = -V_1 \sum_{\langle ij \rangle} \sigma_i \sigma_j - V_2 \sum_{\langle\langle ik \rangle\rangle} \sigma_i \sigma_k - \mu \sum_i \sigma_i, \quad (1)$$

where the first sum is over the four nearest-neighbors, with energy gain $V_1 > 0$, and the second sum, over the four next-nearest-neighbors, has energy interaction $V_2 < 0$ (see Fig.2). The last term in eq.(1) refers to chemical potential contribution μ over all molecules. Here we will consider periodic boundary conditions.

In order to help visualization of the possible phases, the lattice is divided into four sub-lattices: 1, 2, 3, 4 (appropriated for the description of an arbitrary superstructure with twice the lattice spacing of the original lattice). The corners of a simple square are labeled counter-clockwise to indicate the sub-lattices (see example in Fig.3.)

**Figure 1.** Intermolecular interaction**Figure 2.** The neighbor's interactions

The sub-lattice density is given by

$$\rho_\beta = \frac{4}{N} \sum_{j \in \beta} \sigma_j, \quad \beta = 1, \dots, 4. \quad (2)$$

The ground state is defined by the lower grand potential free energy at $T = 0$, and therefore the minimum value of Hamiltonian as given by eq.(1). Due the symmetry of the system, in the case $V_1 > 0$ and $V_2 < 0$, there are two possibilities illustrated below.

2.0.1. If $V_1 < -2V_2$ For $\mu > -3V_1 - 4V_2$ the system stands in the the dense liquid phase (DL), where all sites are occupied. As the chemical potential is decreased, at $\mu = -3V_1 - 4V_2$ there is a phase transition from the dense liquid phase to the structured dilute liquid phase (SDL), illustrated in Fig.3. Decreasing the chemical potential even further, the structured dilute liquid persists until $\mu = -V_1$, where there is a phase transition between the structured liquid and the gas phase. for $\mu < -V_1$, the system stays empty.

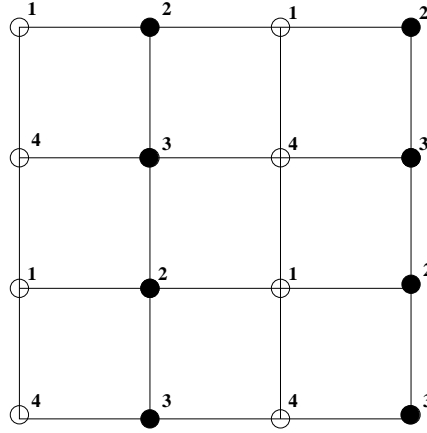


Figure 3. Sub-lattices

2.0.2. If $V_1 > -2V_2$ For $\mu > -2V_1 - 2V_2$ the system is in the dense liquid and for $\mu < -2V_1 - 2V_2$ the stable one is the gas phase. In this case only one phase transition at $\mu = -2V_1 - 2V_2$ is present.

3. Mean-Field Approximation

For the mean field analysis, we will follow a sub-lattice strategy [25] that it is able to capture the phase transition that other mean field schemes miss. The chemical potential can be rewritten as the sum of four potentials, one for each sub-lattice:

$$\mu = \frac{1}{4} \sum_{\alpha=1}^4 \mu_{\alpha}. \quad (3)$$

The use of independent chemical potentials may be necessary in a more general problem, where each sub-lattice is composed by a different type of molecule. For our model we have:

$$\mu_1 = \mu_2 = \mu_3 = \mu_4, \quad (4)$$

which leads, by eq.(3), to

$$\mu = \mu_{\alpha}, \quad \alpha = 1, 2, 3, 4.$$

Now, rewriting the Hamiltonian, eq.(1), in term of the sub-lattices, we get

$$\mathcal{H} = - \sum_{\alpha=1}^4 \sum_{i \in \alpha} H_{\alpha}^{eff}(\{\sigma_j\}) \sigma_i, \quad (5)$$

where

$$H_{\alpha}^{eff}(\{\sigma_j\}) = \mu_{\alpha} + \sum_{\beta=1}^4 \sum_{i \in \beta} J_{ij} \sigma_j, \quad i \in \alpha$$

and where the relation between J_{ij} , V_1 and V_2 is given by:

$$J_{12} = J_{21} = J_{23} = J_{32} = J_{34} = J_{43} = J_{14} = J_{41} = V_1$$

$$J_{13} = J_{31} = J_{24} = J_{42} = V_2.$$

The mean-field approximation here consists in replacing H_α^{eff} by its mean value, given by

$$\langle H_\alpha^{eff} \rangle = \mu_\alpha + \sum_{\beta=1}^4 \sum_{i \in \beta} J_{ij} \langle \sigma_j \rangle, \quad i \in \alpha. \quad (6)$$

Under this approximation, the density of the sub-lattice β is given by $\rho_\beta = \langle \sigma_j \rangle$ and the interaction parameter can be written as

$$\epsilon_{\alpha\beta} = \sum_{i(\neq j)} J_{ij}, \quad i \in \alpha, \quad j \in \beta,$$

what leads to

$$\langle H_\alpha^{eff} \rangle = \mu_\alpha + \sum_{\beta=1}^4 \epsilon_{\alpha\beta} \rho_\beta, \quad i \in \alpha, \quad j \in \beta. \quad (7)$$

Substituting eq.(7) in eq.(5) we get

$$\mathcal{H}^{MF} = - \sum_{\alpha=1}^4 \sum_{i \in \alpha} \left(\sum_{\beta=1}^4 \epsilon_{\alpha\beta} \rho_\beta + \mu_\alpha \right) \sigma_i + \frac{1}{2} \sum_{\alpha=1}^4 \frac{N}{4} \sum_{\beta=1}^4 \epsilon_{\alpha\beta} \rho_\beta \rho_\alpha, \quad (8)$$

where the last term corrects for overcounting. Eq.(8) is the Hamiltonian in the mean-field approximation. With this, we calculate the mean-field grand potential per site, that is

$$\begin{aligned} \phi^{MF} = & -k_B T \ln 2 \\ & - \frac{k_B T}{4} \sum_{\alpha=1}^4 \ln \cosh \left[\frac{1}{2k_B T} \left(\sum_{\beta=1}^4 \epsilon_{\alpha\beta} \rho_\beta + \mu_\alpha \right) \right] \\ & - \frac{1}{8} \sum_{\alpha=1}^4 \left(\sum_{\beta=1}^4 \epsilon_{\alpha\beta} \rho_\beta + \mu_\alpha \right) + \frac{1}{8} \sum_{\alpha=1}^4 \sum_{\beta=1}^4 \epsilon_{\alpha\beta} \rho_\alpha \rho_\beta, \end{aligned} \quad (9)$$

where k_B is the Boltzmann factor and T is the temperature.

The density can be derived from this grand potential as:

$$\rho_\alpha = -4 \left(\frac{\partial \phi^{MF}}{\partial \mu_\alpha} \right)_{T, \mu_{\alpha \neq \beta}}, \quad \alpha = 1, 2, 3, 4,$$

what leads to

$$\rho_\alpha = \frac{1}{2} + \frac{1}{2} \tanh \left[\frac{1}{2k_B T} \left(\sum_{\beta=1}^4 \epsilon_{\alpha\beta} \rho_\beta + \mu_\alpha \right) \right], \quad \alpha = 1, 2, 3, 4, \quad (10)$$

the mean density of a sub-lattice α .

Solving Eqs. (10) for fixed values of temperature and chemical potential it is possible to obtain the density of each sub-lattice and consequently not only the overall density of the system but also specific phase. For instance, if for a given temperature and chemical potential, the sub-lattice densities would be $\rho_1 = \rho_4 = 0$ and $\rho_2 = \rho_3 = 1$, the system would be in structured dilute liquid phase. Since we know that for $T = 0$ two liquid phases exist only if $V_1 < -2V_2$, we explore this region of the parameter space.

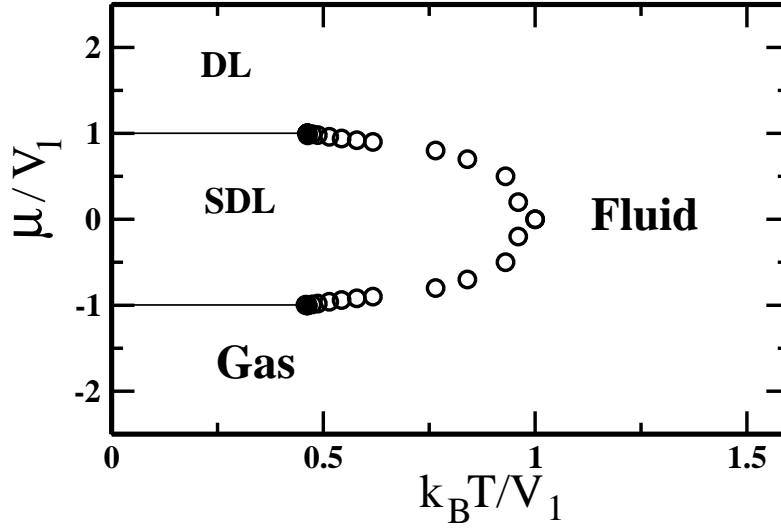


Figure 4. Mean field phase diagram : The open circles represent the second order phase transition, the solid lines are the two first-order phase transitions and the two filled circles are the two tricritical points.

For simplicity, we set $V_1 = 1$ and $V_2 = -1$ (other parameter choices will not affect qualitatively the result) and we construct the mean-field phase diagram shown in Fig. 4.

At high temperatures, each sub-lattice is half full in an disorganized way. This is the fluid phase. As the temperature is lower at a fixed potential $= \mu^* = \mu/V_1 > 1$, all sub-lattices become filled, no phase transition is observed. For very low chemical potentials, $\mu^* < -1$, as the temperature is decreased, the system goes from the fluid to the gas phase continuously with no phase transition. For intermediate chemical potentials, $-1 > \mu^* > 1$, there is a continuous phase transition between the fluid phase and the structured dilute liquid phase. The coexistence line between the gas phase and the structured diluted liquid meets the continuous phase transition at a tricritical point. Another similar point is observed at the contact between the coexistence line between the structured diluted liquid and the dense liquid and the continuous line. The density is monotonic, therefore no density anomaly is observed.

4. Monte Carlo Simulations

The rather simple mean field approach introduced in the previous session is unable to account for the density anomalies. For investigating the possibility of a density anomaly in our potential, Monte Carlo simulations in grand canonical ensemble were performed. The Metropolis algorithm was used to study square $L \times L$ lattice and $|V_2|/V_1 = 1$. Different system sizes $L = 10, 20, 30, 40, 50$ were investigated. The typical equilibration time was 1500000 Monte Carlo time steps for each lattice site.

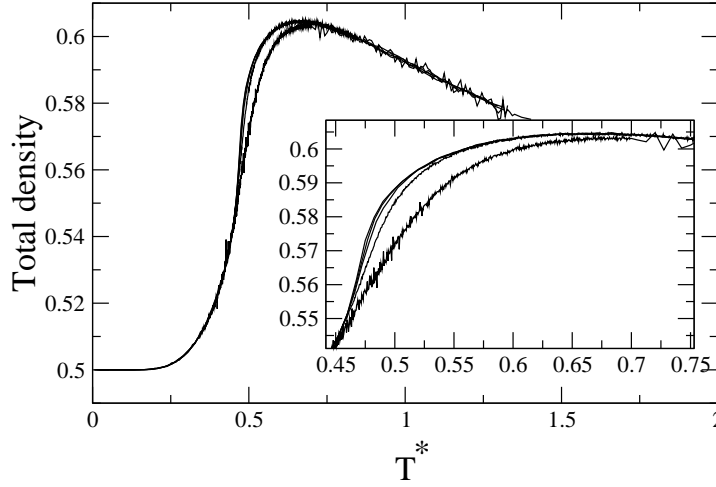


Figure 5. Total density :for the 50, 40, 30, 20 and 10 lattices, from top to bottom.

The nonzero temperature phase-diagram was obtained as follows. For a fixed temperature and chemical potential the density of each sub-lattice and the specific heat was computed by averaging over 5000 measures. Between consecutive measures, τ Monte Carlo steps were performed to decorrelate the system. The *correlation time* τ was calculated using the density correlation function [26]:

$$\chi(t) = \frac{1}{t_{max} - t} \sum_{\tilde{t}=0}^{t_{max}-t} \rho(\tilde{t})\rho(\tilde{t}+t) - \left[\frac{1}{t_{max} - t} \sum_{\tilde{t}=0}^{t_{max}-t} \rho(\tilde{t}) \right] \left[\frac{1}{t_{max} - t} \sum_{\tilde{t}=0}^{t_{max}-t} \rho(\tilde{t}+t) \right]. \quad (11)$$

Fig. 5 shows the total density for the lattice sizes $L = 50, 40, 30, 20$ and 10 , from top to bottom (see also inset) and for fixed chemical potential $\mu^* = 0.5$. According to this graph, one could conclude that no phase transition happens as the temperature is decreased at a fixed chemical potential $\mu^* = 0.5$. However, analyzing the sub-lattice's densities illustrated in Figs. 6 - 9 (here we are illustrating only the result obtained for the $L = 20$), it's clear from the strong density fluctuations that appear at $T^* = T/V_1 = 0.45$ a phase transition occurs. The peak in the specific heat shown in Fig. 10 confirms the existence of this transition and helps to determined the exact location of the critical point T_c^* .

The energy histograms constructed for fixed temperatures around the critical temperature T_c^* are shown in Figs. 11-13. For temperatures above and below T_c^* , there is only one peak indicating that the transition is continuous (two peaks would be a signature of first-order transition).

Analyzing again Figs. 6 - 9 it can be seen that for $T^* > 0.45$ the sub-lattice densities $\rho_\beta \approx 0.56$, indicating that the system is in the fluid phase. For $T^* < 0.45$, $\rho_1 = \rho_2 = 0$ and $\rho_3 = \rho_4 = 1$, that is a signature of the structured dilute liquid. Hence, it is clear that around $T_c^* = 0.45$ there is a continuous transition between the fluid and the SDL

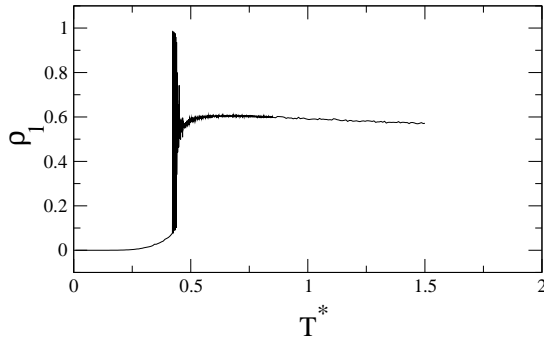


Figure 6. Sub-lattice 1

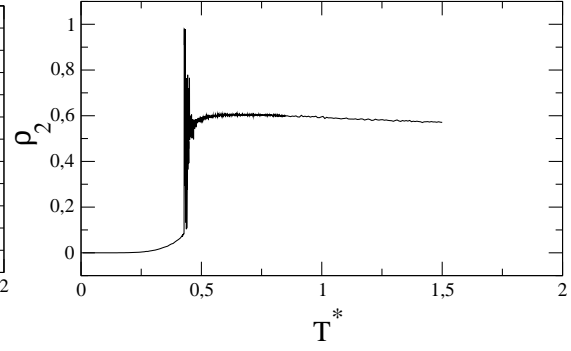


Figure 7. Sub-lattice 2

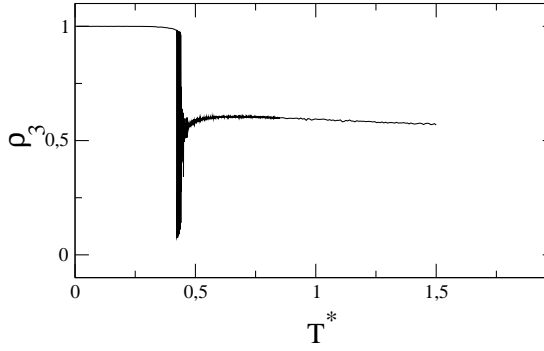


Figure 8. Sub-lattice 3

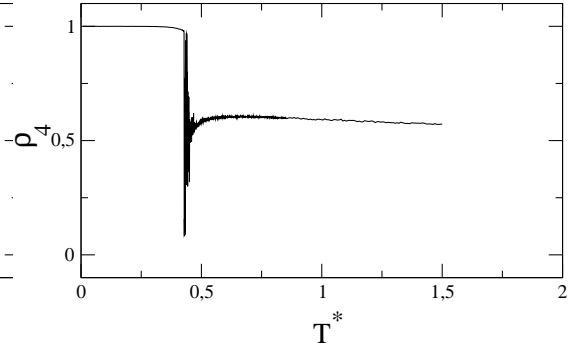
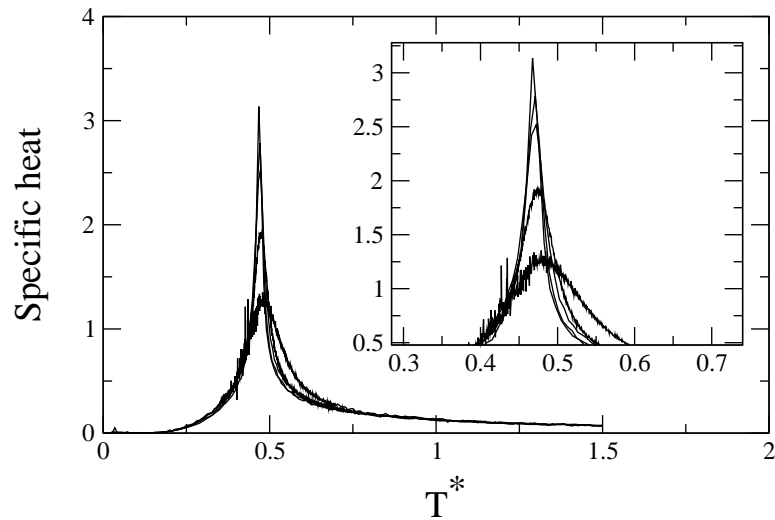


Figure 9. Sub-lattice 4


 Figure 10. Specific heat for $\mu^* = 0.50$ and $L = 50, 40, 30, 20, 10$ from top to bottom.

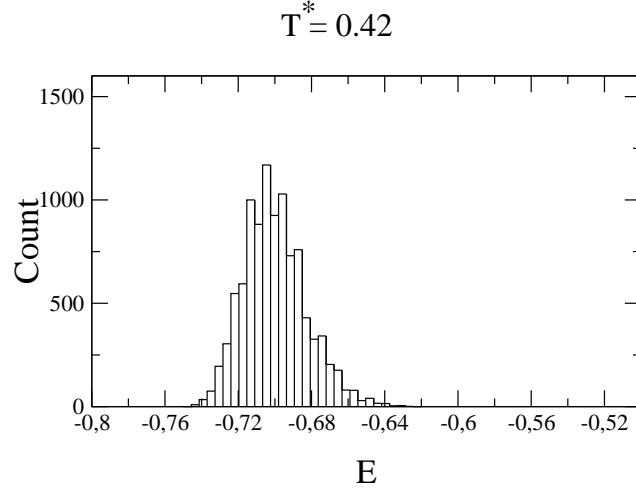


Figure 11. Energy histogram for $T < T_c$, $\mu^* = 0.50$ and $L = 20$

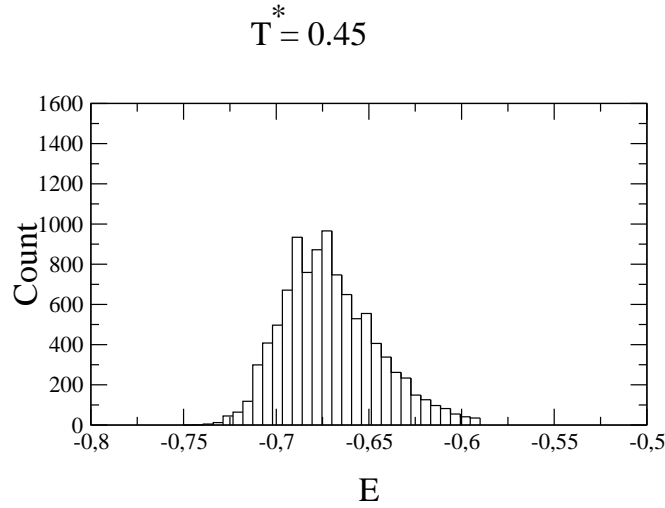


Figure 12. Energy histogram for $T \approx T_c$, $\mu^* = 0.50$ and $L = 20$

phases. The error bars associated with the location of the critical temperatures for the lattice sizes $L = 10, 20$ are respectively $\Delta T = 4 \times 10^{-4}$, $\Delta T = 7.5 \times 10^{-3}$ while for the lattice size $L = 30, 40, 50$ is given by $\Delta T = 6.5 \times 10^{-3}$.

Criticality happens only in the thermodynamic limit. Therefore in order to determined the actual critical temperature, it is necessary to extrapolate the results obtained for the finite system to the limit of $L \rightarrow \infty$. The critical temperature for the finite system can be obtained: from the maximum of the specific heat or from the minimum of the fourth order Binder's cumulant V_E [27]. This last method requires computing for each lattice size, the quantity:

$$V_E = 1 - \frac{\langle E^4 \rangle}{3 \langle E^2 \rangle^2} \quad (12)$$

where E is the total energy of the system.

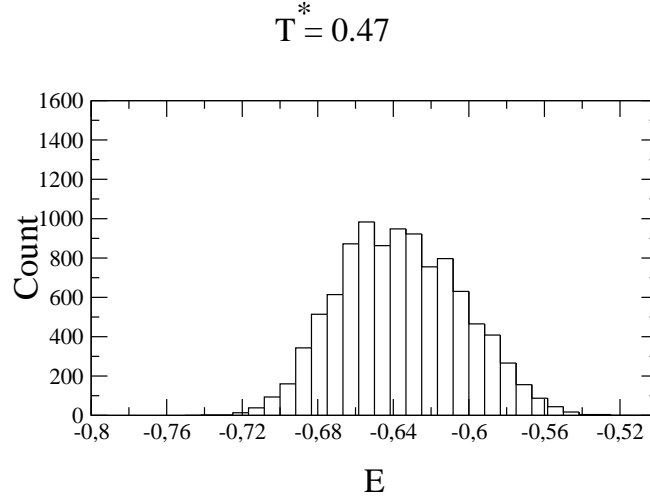


Figure 13. Energy histogram for $T > T_c$, $\mu^* = 0.50$ and $L = 20$

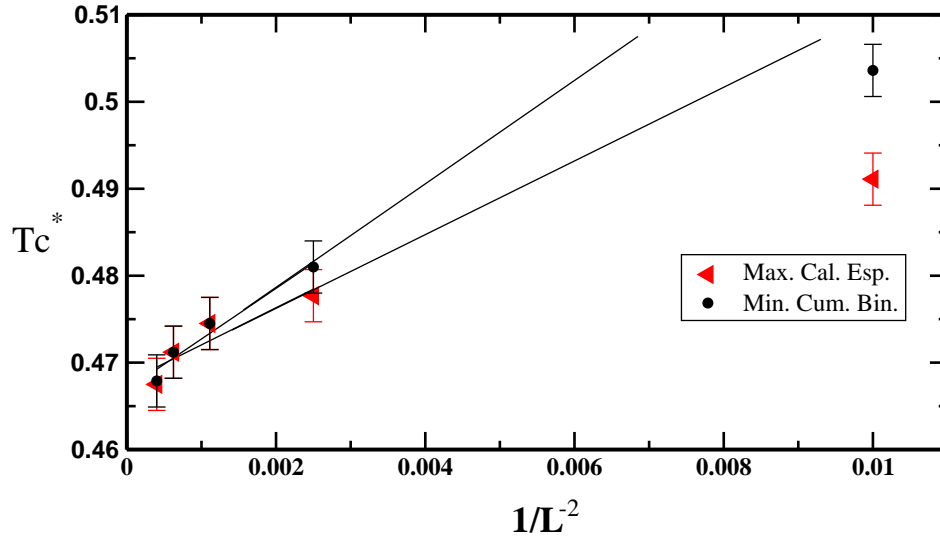


Figure 14. $T_c^* \times 1/L^2$ for $L = 10, 20, 30, 40, 50$. The circles are the minimum of Binder's cumulant and the triangles are the maximum of specific heat.

Fig. 14 shows the critical temperature of the finite system for different lattice sizes obtained from the two methods refereed above. The extrapolation to $1/L \rightarrow 0$ gives the critical temperature for the infinite system. The values obtained from the peak of the specific heat and from the minimum of the Binder's forth order cumulant are respectively 0.467 and 0.466. The difference between the two results is smaller than the error on the calculation of both numbers. The lattice $L = 10$ was excluded from the extrapolation because it is so far from the infinite size limit that its inclusion would require carrying nonlinear terms into the extrapolation.

Fig. 5 shows that for a fixed chemical potential the density has a maximum at a certain temperature T_{max} . The temperature of maximum density as a function of the

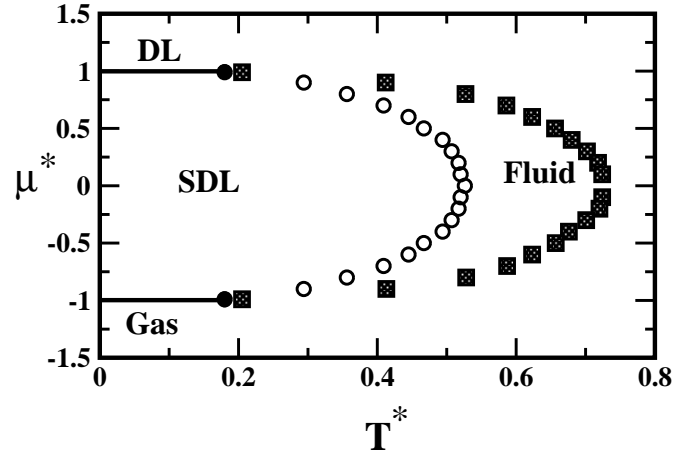


Figure 15. $\mu^* \times T^*$ phase-diagram : the circles indicates the critical line, the solid lines show the first-order transitions, the squares locate the temperature of maximum density and the full circles are the tricritical points. The error bars are smaller than the symbols.

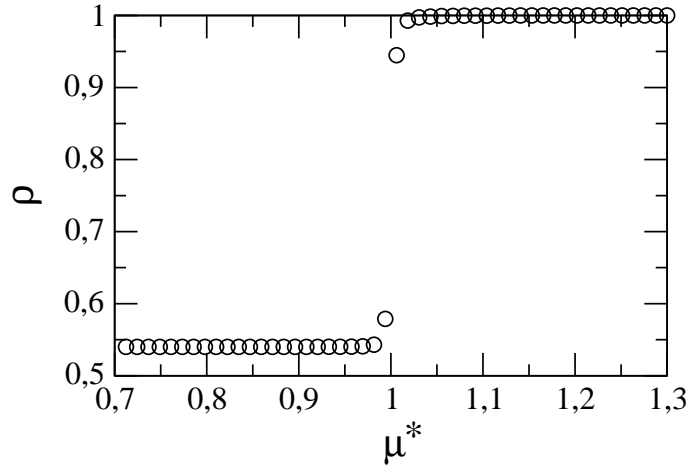


Figure 16. $\rho \times \mu^*$ for $T^* = 0.19$

chemical potential is illustrated on Fig. 15.

In order to observe the first-order phase transitions between the gas and SDL phase and between the SDL phase and the DL phase, simulations at fixed temperature and varying the chemical potential were performed. Figure 16 shows that for $T^* = 0.19$ the transition between the SDL and the DL happens at $\mu^* = 1$. At low chemical potentials similar transition is observed between the gas and the SDL phases. At the intersection between the critical line and the first-order phase transition lines arise two tricritical points as indicated in Fig. 15.

By integrating the the Gibbs-Duhem relation:

$$SdT - Vdp + Nd\mu = 0, \quad (13)$$

where S stands for entropy and p for pressure, together with the MC simulations at a

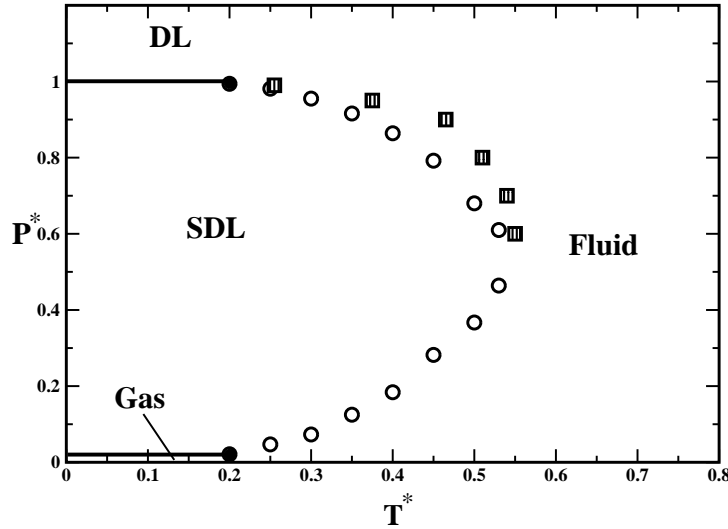


Figure 17. $p^* \equiv p/|V_1| \times T^*$ phase diagram : the solid lines indicate first-order transitions, the empty circles locate the continuous line, the squares show the temperature of maximum density and the filled circles are the tricritical points. The error bars are smaller than the symbols.

fixed temperature, the dependence of the pressure on the density for a fixed temperature was obtained. Comparing this dependence for different temperatures, was possible to extract the phase-diagram illustrated at Fig.17. Here the density anomaly appears as the temperature of maximum density for a fixed pressure.

The phase-diagram for other values of $V_1 < -2V_2$ is similar to the one we present here. In the case of $V_1 > -2V_2$ both the two liquid phases and the density anomaly are not present.

5. Conclusions

The phase-diagram of a two dimensional lattice gas model with competing interactions and in contact with a reservoir of particles and temperature was investigated with the purpose of testing this attraction/repulsion potential for the presence of criticality and density anomaly .

This system exhibits two liquid phases and a line of density anomalies. Differently from the general belief, the density anomaly line in the present case is not associated to a single critical point [9] but with a line of critical points. Besides, the density anomaly does not arise from a softened core potential but from an outer shell repulsion that competes with a short-range attraction. We believe that the common ingredient that leads to the presence of demixing between two liquid phases both in softened core potentials and in the present model is the existence of two competing scales for the interaction [29][28].

The relation between the form of the potential, criticality and the density anomaly goes as follows. The presence of two liquid phases comes from the presence of competing

scales. While the short-range attraction favors the formation of a dense liquid phase, the outer shell repulsion favors the formation of an open structure, the SDL phase.

In systems dominated by short-range attractive forces, if the pressure is kept fixed, the density increases on cooling. In our case, similar behavior is only observed at high temperatures where short-range interactions are dominant. As the temperature is decreased, the outer shell repulsion prevents the density to increase beyond a certain limit. Therefore, the same competition responsible for the appearance of two liquid phases leads to the density anomaly.

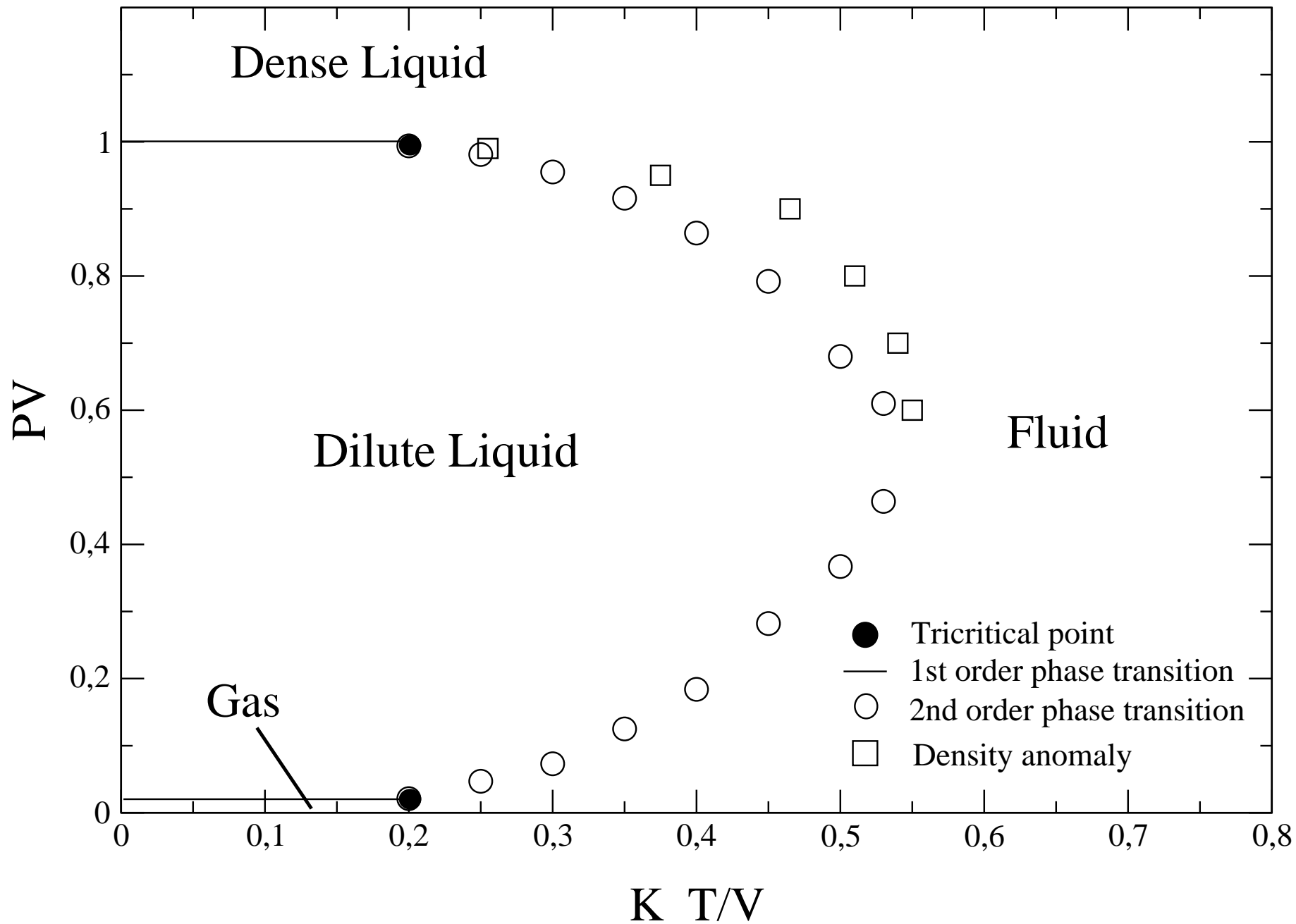
One should point out that the presence of a critical line instead of a single critical point as one could generally expect [9] is not surprising. Due to the lattice structure, the SDL is not one single phase but the region where two different phases coexist (empty/full rows and empty/full columns). These two phases become critical together with the DL phase at the tricritical point that is also the locus where critical line ends.

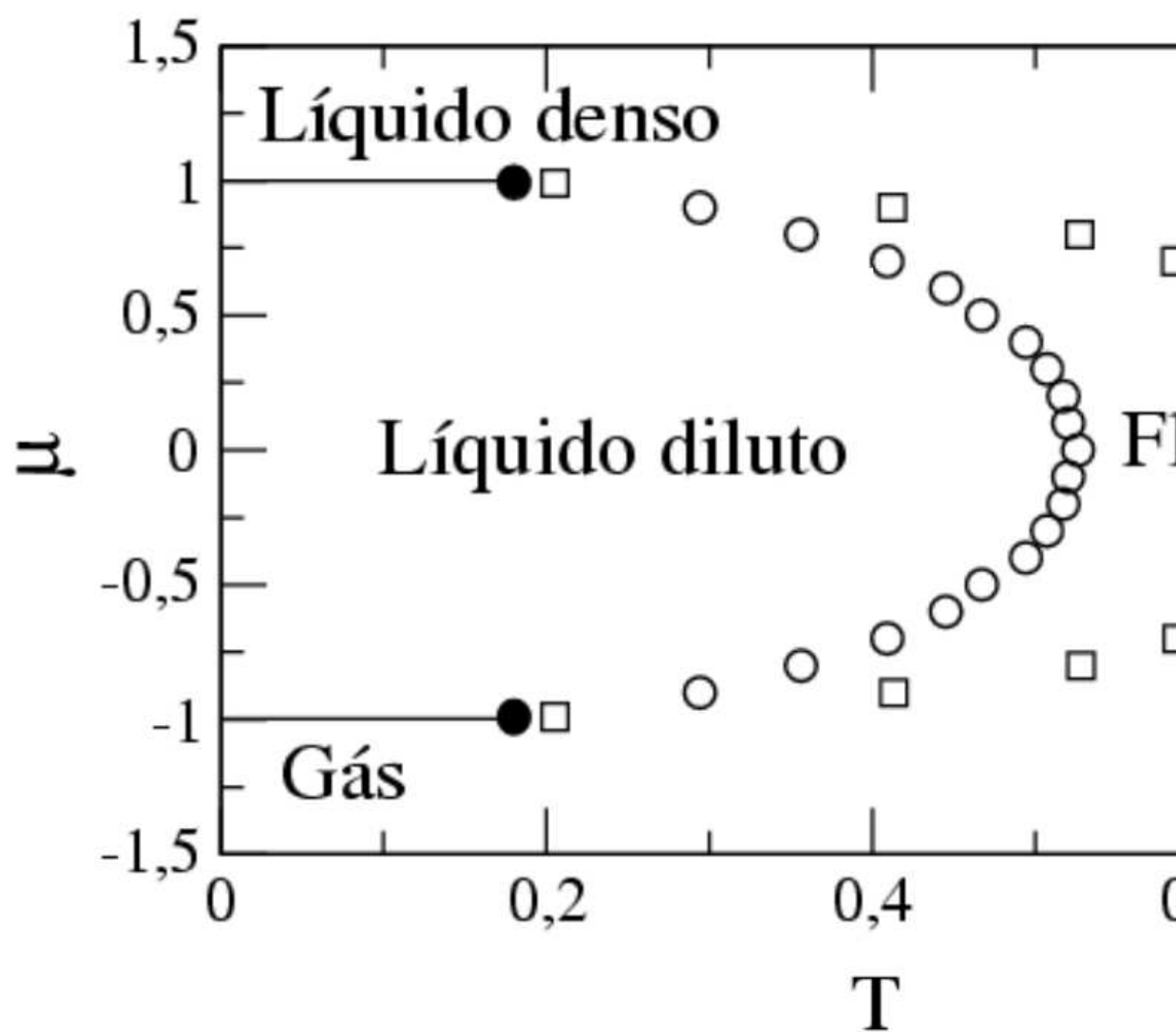
Acknowledgments

This work was supported by the Brazilian science agencies CNPq, FINEP, Capes and Fapergs.

- [1] R. Waller, *Essays of Natural Experiments*, Johnson Reprint corporation, New yourk , 1964.
- [2] F. X. Prielmeir, E. W. Lang, Rl. Speedy, H. -D. Lüdemann, *Phys. Rev. Lett.* **59**, 1128 (1987).
- [3] F. X. Prielmeier, E. W. Lang, R. J. Speedy, H. -D. Lüdemann, B. Bunsenges, *Phys. Chem.* **92**, 1111 (1988).
- [4] L. Haar, J. S. Gallagher, G. S. Kell, *NBS/NRC Steam Tables. Thermodynamic and Transport Properties and Computer Programs for Vapor and Liquid States of Water in SI Units*, Hemisphere Publishing Co., Washington DC, 1984, pp271-276.
- [5] Paulo A. Netz, Francis W. Starr, H. E. Stanley, and Marcia C. Barbosa, *J. of Chem. Phys.* **115**, 344 (2001).
- [6] P. G. Debenedetti, *Metastable Liquid*, Princeton University Press, Princeton, 1996.
- [7] O. Mishima, H. E. Stanley, *Nature* **396**, 329 (1998).
- [8] Y. Yoshimura, B. Bunsenges, *Phys. Chem.* **95**, 135 (1991).
- [9] P.H. Poole, F. Sciortino, U. Essmann, and H. E. Stanley, *Nature* **360**, 324 (1992); *Phys. Rev. E* **48**, 3799 (1993); F. Sciortino, P.H. Poole, U. Essmann, and H.E. Stanley, *Ibid* **55**, 727 (1997); S. Harrington, R. Zhang, P.H. Poole, F. Sciortino, and H.E. Stanley, *Phys. Rev. Lett.* **78**, 2409 (1997).
- [10] R.J. Speedy and C.A. Angell, *J Chem Phys* **65**, 851 (1976).
- [11] O. Mishima, L. D. Calvert and E. Whalley, *Nature* **310**, 393 (1984).
- [12] R. S. Smith and B D. Kay, *Nature* **398**, 788 (1999).
- [13] O. Mishima and Y. Suzuki, *Nature (London)* **419**, 599 (2002); R. Martonak, D. Donadio and M. Parrinello, *Phys. Rev. Lett.* **92**, 225702 (2004).
- [14] Y. Katayama, T. Mizutani, W. Utsumi, O. Shimomura, M. Yamakata and K. Funakoshi, *Nature* **403**, 170 (2000).
- [15] G. Monaco, S. Falconi, W.A. Crichton and M. Mezouar, *Phys. Rev. Lett.* **90**, 255701 (2003).
- [16] D.J. Lacks, *Phys. Rev. Lett.* **84**, 4629 (2000).
- [17] P. T. Cummings and G. Stell, *Mol. Phys.* **43**, 1267 (1981).
- [18] M. Togaya, *Phys. Rev. Lett* **79**, 2474 (1997).
- [19] G. Franzese, G. Malescio, A. Skibinsky, S. V. Buldyref and H. E. Stanley, *Nature* **409**, 692 (2001).

- [20] P. C. Hemmer and G. Stell, Phys. Rev. Lett. 24, 1284 (1970); G. Stell, P. C. Hemmer, J. Chem. Phys. 56, 4274 (1972).
- [21] J. S. Hoye, P. C. Hemer, Physica Norvegica 7, 1 (1973).
- [22] P. G. Debenedetti, V. S. Raghavan, S. S. borick, J. Phys. Chem. 95, 4540 (1991).
- [23] M. R. Sadr-Lahijany, A. Scala, S. V. Buldyrev, and H. E. Stanley, Phys. Rev. Lett. 81, 4895 (1998).
- [24] A. Scala, F. W. Starr, E. La Nave, H. E. Stanley and F. Sciortino, Phys. Rev. E 62, 8016 (2000).
- [25] K. Binder and D. P. Landau, Phys. Rev. B 21, 1941 (1980)
- [26] M. E. J. Newman and G. T. Barkem, Monte Carlo methods in statistical physics. Oxford, Clarendon Press, 1999.
- [27] Shan-ho Tsai and S. R. Salinas, Braz. J. Phys. 28, 58 (1998).
- [28] Vera B. Henriques and Marcia C. Barbosa, "Liquid Polymorphism and Density Anomaly in a Lattice Gas Model", submitted.
- [29] Aline Lopes Balladares and Marcia C. Barbosa, " Density Anomaly in Core-Softened Lattice Gas ", submitted.





— Transição de 1º ordem ● Ponto crítico
 ○ Transição de 2º ordem □ Anomalia